HHS Public Access

Author manuscript

Biomaterials. Author manuscript; available in PMC 2017 May 01.

Published in final edited form as:

Biomaterials. 2016 May ; 87: 82–92. doi:10.1016/j.biomaterials.2016.02.008.

Enhanced biocompatibility of CD47-functionalized vascular stents

Joshua B. Slee[a,b], **Ivan S. Alferiev**[a,b], **Chandrasekaran Nagaswami**[c], **John W. Weisel**[c], **Robert J. Levy**[a,b], **Ilia Fishbein**[a,b,*], and **Stanley J. Stachelek**[a,b,*]

[a] Division of Cardiology-Department of Pediatrics, The Children's Hospital of Philadelphia

[b] Perelman School of Medicine, The University of Pennsylvania

[c] Department of Cell and Developmental Biology, Perelman School of Medicine, The University of Pennsylvania

Abstract

The effectiveness of endovascular stents is hindered by in-stent restenosis (ISR), a secondary re-obstruction of treated arteries due to unresolved inflammation and activation of smooth muscle cells in the arterial wall. We previously demonstrated that immobilized CD47, a ubiquitously expressed transmembrane protein with an established role in immune evasion, can confer biocompatibility when appended to polymeric surfaces. In present studies, we test the hypothesis that CD47 immobilized onto metallic surfaces of stents can effectively inhibit the inflammatory response thus mitigating ISR. Recombinant CD47 (recCD47) or a peptide sequence corresponding to the Ig domain of CD47 (pepCD47), were attached to the surfaces of both 316L-grade stainless steel foils and stents using bisphosphonate coordination chemistry and thiol-based conjugation reactions to assess the anti-inflammatory properties of CD47-functionalized surfaces. Initial *in vitro* and *ex vivo* analysis demonstrated that both recCD47 and pepCD47 significantly reduced inflammatory cell attachment to steel surfaces without impeding on endothelial cell retention and expansion. Using a rat carotid stent model, we showed that pepCD47-functionalized stents prevented fibrin and platelet thrombus deposition, inhibited inflammatory cell attachment, and reduced restenosis by 30%. It is concluded that CD47-modified stent surfaces mitigate platelet and inflammatory cell attachment, thereby disrupting ISR pathophysiology.

Introduction

Although there has been remarkable progress in prevention, diagnostics, and treatment, atherosclerosis remains the leading cause of death in our society. A recent report from the American Heart Association showed that 15.5, 6.8, and 6.6 million Americans are affected

*Co-senior authors and Address Correspondence to Stanley J. Stachelek, Ph.D., Children's Hospital of Philadelphia, Abramson Research Building, 3615 Civic Center Blvd., Suite 702, Philadelphia, PA 19104-4318, Telephone: (215) 590-0157, stachelek@email.chop.edu; Ilia Fishbein, M.D., Ph.D., Children's Hospital of Philadelphia, Abramson Research Building, 3615 Civic Center Blvd., Suite 702, Philadelphia, PA 19104-4318, Telephone: (215) 590-8740, fishbein@email.chop.edu.

by coronary heart disease, peripheral artery disease, and cerebrovascular disease, respectively, with a combined yearly toll of more than 400 thousand lives due to these conditions [1]. Stent angioplasty is now the definitive first line therapy for occlusive vascular disease. However, in-stent restenosis (ISR) presents a formidable problem, only partially addressed using drug-eluting stents (DES)[2, 3], which perform sub-optimally in patients with renal failure, diabetes, and patients with smaller vessel diameters[4]. Moreover, by inhibiting re-growth of endothelium, DES increase the incidence of late stent thrombosis[5]. Additionally, the economic burden of ISR is at least $2.8 billion a year in the United States alone[6]. Therefore, a strategy based on alleviating the molecular and cellular events triggered by stent deployment could provide a viable strategy for reducing the clinical and financial toll of ISR.

Several lines of evidence indicate that initial interactions of blood-borne cells with metal surfaces of stents initiates a pro-inflammatory and pro-thrombotic cascades that largely contribute to the subsequent neointimal growth by creating a persistent, positive feedback mechanism of cell recruitment, intimal migration, and proliferation supported by the cytokines and growth factors released by the stent-associated cells[7-10]. To this end, researchers have focused on diminishing inflammatory cell binding to the stents[11-13]. These strategies, which are often based on establishing a bioinert coating at the blood-material interface, are not entirely effective, and improving stent biocompatibility remains an unmet need in cardiovascular device development. Motivated by the lack of strategies to improve upon the biocompatibility of medical devices, our group has investigated the use of recombinant CD47, a ubiquitously expressed transmembrane protein, that when bound to its cognate receptor, Signal Regulatory Protein alpha (SIRPα), functions as a molecular marker of self, that reduces the material-induced inflammatory response. We have shown that inflammatory cell attachment and activation was significantly reduced when CD47-functionalized surfaces were tested *in vitro*, *ex vivo*, and *in vivo* [14-16], and that platelet activation and attachment were also reduced when blood was exposed to CD47-functionalized surfaces [14]. As shown previously by others, reducing aberrant blood interactions with damaged arterial walls post angioplasty enhances arterial healing and ultimately improves outcomes [17]. Thus, we hypothesize that CD47-functionalized metallic surfaces would enhance stent biocompatibility by reducing pro-thrombotic and pro-inflammatory events that are regularly seen when blood is exposed to synthetic surfaces.

The use of a CD47 based anti-inflammatory strategy is further strengthened by recent findings pertaining to the molecule's bioactive region. Specifically, it has been reported that a peptide sequence corresponding to the extracellular Ig domain of CD47 can bind SIRPα [18]. Peptides tend to be more biocompatible and less costly to manufacture in contrast to the more complex production of recombinant proteins [19-21]. Compared to recombinant proteins, peptides can be more easily modified and thus more amenable to a range of functionalization chemistries used to append therapeutic molecules to biomaterial surfaces [19-21]. Thus, investigations into the effectiveness of pepCD47 in reducing the aberrant host response to endovascular stents could provide a cost-effective therapeutic means to address ISR.

Central to our strategy of fabricating CD47 functionalized surfaces is a recently developed chemical modification that enables the covalent immobilization of a range of therapeutic modalities on metallic surfaces. This strategy proved effective in immobilizing adenoviral vectors on polyallylamine bisphosphonate-modified uncoated stainless steel surfaces of endovascular stents [22, 23]. A water-soluble polyallylamine bisphosphonate (PAB) was shown to create an ultra-thin (< 5 nm) monolayer arrangement on the surface of stainless steel and other alloys used in stent manufacture due to the formation of coordination bonds between the bisphosphonic groups and the metals and metal oxides of the metal surfaces [23]. Introduction of latent thiol groups into polyallylamine chains as realized in PABT [22] renders metal surface amenable to further modification using well characterized thiol chemistry [24]. This "coatless" method of generating a thiolated stent surface was further combined with our published chemistry utilized to append CD47 to polymeric surfaces [14-16]. Here, we show that using this PABT modification is a feasible method to functionalize steel stents with CD47, which we further show prevents acute thrombosis and chronic inflammation as well as restenosis *in vivo* in a rat model.

In these present studies, we tested the hypothesis that immobilized CD47 can significantly reduce the inflammatory response observed during stent deployment. The goals of these studies were as follows: 1. Develop and characterize a surface modification strategy to covalently append CD47 to metallic surfaces, 2. Perform comparative analysis of the anti-inflammatory capacity of immobilized full-length recombinant CD47 and CD47-derived peptide, 3. Demonstrate that immobilized CD47 can inhibit ISR in an *in vivo* model.

1. Materials and Methods

1.1. Materials

Clinical grade polyvinyl chloride (PVC) tubing conduits were acquired from Terumo Cardiovascular Systems (Ann Arbor, MI). Stainless steel (AISI 316L) foils (100 mm × 100 mm × 0.05 mm) were obtained from Goodfellow (Coraopolis, PA) and stainless steel (AISI 316L) inserts (1 cm × 5 mm ID × 7 mm OD) designed to fit inside the Terumo PVC tubing conduits were obtained from Microgroup (Medway, MA). Stainless steel stents (AISI 304), 1mm diameter, were made by Laserage (Waukegan, IL) [22]. Sulfo-NHS-LC-LC-Biotin, sulfo-long chain-N-succinimidyl 3[2-pyridyldithio]-propionate (Sulfo-LC-SPDP), dithiothreitol (DTT), Ultra TMB (3,3',5,5'-tetramethylbenzidine) Substrate, tris (2-carboxyethyl) phosphine hydrochloride (TCEP), 16% formaldehyde, and 2-mercaptoethanol were obtained from Thermo Scientific (Waltham, MA). Sulfo-NHS-Acetate was obtained from G Biosciences (St. Louis, MO). Bovine serum albumin (BSA) and Triton-X-100 were obtained from Sigma (St. Louis, MO). Dulbecco's phosphate buffered saline (DPBS) was obtained from Gibco (Grand Island, NY). 4', 6-diamidino-2-phenylindole (DAPI)-containing Vectashield mounting media was obtained from Vector Labs (Burlingame, CA). 25% glutaraldehyde was obtained from Alfa Aesar (Ward Hill, MA).

Recombinant CD47 (recCD47) with a poly-lysine C-terminal domain was produced and purified as previously described [14]. A peptide encompassing the extracellular Ig domain of human CD47 (pepCD47) was synthesized with the addition of a poly-lysine tail (Ac-Gly-Asn-Try-Thr-Cys-Glu-Val-Thr-Glu-Leu-Thr-Arg-Glu-Gly-Glu-Thr-Ile-Ile-Glu-Leu-Lys-

AEEAc-Lys-Lys-Lys-Lys-Lys-Lys-Lys-Lys-OH) by Bachem (Torrance, CA). A thiolated peptide derived from the extracellular Ig domain of rat CD47 (Ac-Gly-Asn-Tyr-Thr-Cys-Glu-Val-Thr-Glu-Leu-Ser-Arg-Glu-Gly-Lys-Thr-Val-Ile-Glu-Leu-Lys-AEEAc-AEEAc-Cys-OH) and its scrambled variant (Ac-Gly-Cys-Thr-Glu-Val-Asn-Leu-Ile-Lys-Leu-Ser-Gly-Arg-Val-Tyr-Glu-Thr-Glu-Glu-Thr-Lys-AEEAc-AEEAc-Cys-OH) were also synthesized by Bachem.

1.2. Functionalizing Steel with CD47

As depicted in Figure 1, steel surface functionalization chemistry was adapted based on our previous work tethering adenoviral vectors to vascular stents [22, 23, 25]. Briefly, 316L-grade steel foil samples or 304 grade stents (1mm diameter) were cleaned with isopropanol and nitric acid and exposed to 1% aqueous solution of polallylamine bisphosphonate with latent thiol groups, PABT as previously described [22]. We have shown that this treatment creates a stable polymer monolayer on the steel surface due to the formation of coordination bonds between Fe and Cr atoms on the metal surface and bisphosphonic groups of the polymer [23]. After thiol group deprotection by TCEP (12 mg/ml in 0.1 M acetic buffer at 28°C for 10 min) and washing in degassed double distilled water, the PABT-modified surfaces were reacted with 2% polyethyleneimine (PEI) with installed pyridyldithio groups (PDT) for amplification of attachment sites (PEI-PDT [19]) at 28°C for 1h and washed in double distilled water. Finally, PDT groups on the metal surface were converted into thiols with DTT (10 mg/ml at 4°C for 10 min) priming the steel surface for the conjugation with thiol-reactive CD47 moieties. Thiol-reactive recCD47, pepCD47, and BSA (control) were prepared by reaction with Sulfo-LC-SPDP (10 mg/ml at 28°C for 45 min). Unreacted SPDP was removed by desalting proteins through a 7 kDa cutoff column. Purified thiol-reactive recCD47, pepCD47, and BSA were then incubated with the thiol-installed metal surfaces overnight at 28°C in an argon atmosphere and subsequently rinsed/stored in DPBS. This process is summarized schematically in Figure 1. For the attachment of thiolated pepCD47 or thiolated scrambled control peptide, no DTT reduction of PEI-PDT and SPDP linker chemistry are required. Therefore, the modification chemistry was processed up to PEI-PDT addition. The thiolated scrambled control peptide and the thiolated pepCD47 were then directly reacted with the PEI-PDT-modified steel.

1.3. Quantification of Appended CD47

The same sequence of surface modification reactions as described in 2.2 was used to assemble a monolayer of PABT on the surface of stainless steel foils of a known surface area and to expand the thiol-reactive capacity of the surface with a PEI-PDT amplifier. Once PEI-PDT was appended, the surfaces were reacted with sulfo-NHS-acetate (2.5 mg/ml in carbonate bicarbonate buffer at 28°C for 45 min) to cap all primary amines present in PABT and PEI-PDT by acylation. Next, PDT groups on the surface were converted to thiols with a 10 min DTT exposure (10 mg/ml in degassed distilled water at 4°C) followed by reaction with sulfo-LC-SPDP [5 mg/ml in degassed dimethylformamide (DMF)] at 28°C with shaking for 1 hour. Since no amines are accessible on the steel surface after sulfo-NHS-acetate conjugation, sulfo-LC-SPDP is tethered to the surface through the reaction of PDT moiety with the surface-exposed thiol groups, leaving amino-reactive NHS ends available for further modification. Concurrently with the modification of steel samples, 500 μg of pepCD47 were dissolved in 600 μl of DMF and 5 μl of trimethylamine, and reacted with 100 μl of 2 mg/ml EZ-Link sulfo-NHS-LC-LC-biotin in DMF. Similarly, 200 μl of 12 mg/ml recCD47 with C-terminal poly-lysine domain were diluted with 200 μl of CCB and reacted with 300 μl of 2 mg/ml EZ-Link sulfo-NHS-LC-LC-biotin in DMF. The amounts of biotinylation reagent were calculated to modify on average 1 out of 9 and 8 out of 10 lysine residues present in the tagged poly-lysine tails of pepCD47 and recCD47, respectively. Both reactions were carried out at 28°C with shaking for 1 hour. Without further purification, the reaction mixtures were added to the sulfo-LC-SPDP-activated steel foil samples to append biotinylated pepCD47 and recCD47. This final conjugation step was carried out at 28°C with shaking for 2 hours. The groups of similarly prepared foils, treated with 600 μl of 1 mg/ml bovine serum albumin in DMF or non-treated beyond sulfo-LC-SPDP activation were used as controls. To quantify biotin on the metal surface, the foil samples were individually placed in the wells of a 96-well plate with 100 μl 1:50 dilution of ABC reagent (Vector Labs, Burlingame, CA) consisting of stoichiometric amounts of avidin and biotinylated peroxidase in 1% BSA/PBS for 25 min, followed by thorough PBS washing. Finally, Ultra TMB substrate (Thermo Scientific) was added per manufacturer recommendation to determine the relative concentrations of surface-immobilized biotin. The absolute values of CD47 immobilization density were obtained by plotting the OD data generated with the sets of foil samples to a standard OD curve obtained with escalating amounts of biotinylated goat anti-rabbit antibody (Vector Lab), disclosed to contain an average of 10 biotin groups per a 150 kDa molecule. In a separate experiment the contribution of non-covalent binding of CD47 to the PEI-PDT modified steel surfaces was assessed by omitting both the reduction of PDT groups with DTT and subsequent surface modification with sulfo-LC-SPDP.

1.4. Cell Culture

A human monocyte-derived macrophage (THP-1) cell line was obtained from ATCC (Manassas, VA) and maintained as recommended by the supplier. THP-1 cells grown in RPMI-1640 media supplemented with 5% fetal bovine serum and 0.05 μM 2-ME. Where indicated cells were differentiated, as previously described [16], with the addition of 1.6×10^{-7}M of phorbol 12-myristate 13-acetate (PMA) (Sigma) to the media. Human Umbilical Vein Endothelial Cells (HUVECs) were obtained from ATCC (Manassas, VA) and were maintained in EGM-2 Bullet Kit supplemented basal cell culture media (Lonza, Walkersville, MD). HUVECs were maintained and used prior to passage 10 for shear stress experiments.

1.5. In Vitro THP-1 Attachment Studies

THP-1 cells were differentiated with the addition of PMA to their media and were cultured on bare metal steel foils, BSA, recCD47, or pepCD47-modified steel foils for 3 days. After 3 days, the foils were gently rinsed with DPBS, fixed with 4% formaldehyde, and stained with the nuclei specific stain, DAPI. DAPI staining of adhered cells was visualized using a fluorescent microscope with the appropriate filter set and randomly selected 200X fields were visualized and counted for statistical significance.

1.6. In Vitro HUVEC Fluid Shear Stress

HUVECs were cultured on stainless steel foils which were cut to match the dimensions of FlexCell® Streamer® slides (Flexcell International Corp., Burlington, NC) for use with the FlexCell® Streamer® Shear Stress device. HUVECs were seeded on stainless steel foils and cultured to confluency. Once confluent, the HUVECs were exposed to 25 dynes/cm^2 shear stress for 4 hr using the FlexCell® Streamer® device as previously described [26]. Following shear stress exposure the HUVECs were fixed with 4% formaldehyde overnight at 4°C. After overnight fixation, the cells were permeabilized with 0.1% Triton-X-100 for 15 min at room temperature. Actin stress fibers were then stained with rhodamine-Phalloidin (Life Technologies, Grand Island, NY) for 30 min at room temperature, following which the nuclei were DAPI stained for 30 min prior to imaging. HUVECs were imaged using a fluorescent microscope fitted with the necessary filter sets under 200X magnification.

1.7. Chandler Loop Apparatus Experiments

As described previously [14, 16], the Chandler Loop apparatus was used to expose whole human or rat blood to the luminal surface of unmodified steel inserts or BSA, recCD47, or pepCD47-modified steel inserts which were inserted into medical grade PVC tube conduits. Human blood was obtained via venipuncture from healthy volunteers under an IRB approved protocol and rat blood was collected from sacrificed rats following an IACUC approved protocol at The Children's Hospital of Philadelphia. Briefly, 10 ml of citrate-treated whole blood (human) or heparinized whole blood (rat) were perfused through the tubing for 3 hr at a shear rate of 28 dynes/cm^2. At the end of the 3 hr, the blood samples were withdrawn and the steel inserts were removed and gently rinsed with DPBS. Steel inserts were fixed with 4% formaldehyde overnight at 4°C for cell counting. For imaging, the steel inserts were cut open using tin snips and flattened using a mechanical press. Nucleated cells were stained with DAPI as described for the shear stress experiments. Nine randomly selected fields of view under 200X magnification were counted and statistical analyses were performed. Representative images were taken from these nine random fields.

1.8. Rat Carotid Stent Angioplasty

Rat stent procedures were performed as previously reported [25]. All animal procedures conformed to federal regulations on laboratory animal use and were approved by the IACUC of the Children's Hospital of Philadelphia. The animals were euthanized at predetermined time points, and the harvested stented segments of common carotid arteries were gently flushed with heparinized saline prior to 4% formaldehyde or 2% glutaraldehyde fixation. Therapeutic and mechanistic studies investigating stenting-induced neointimal formation and inflammatory cell recruitment to the stented arteries, respectively, used 10 and 4 rats per treatment group. There were 2 preterm euthanasia cases in the therapeutic study urged by humane considerations (one in the CD47 stent group, and one in the control stent group; both on day 2 post-surgery due to respiratory complications). These rats were excluded from the analysis.

1.9. Scanning Electron Microscopy (SEM)

Following explantation, stents were cut along their long axis and gently opened to expose the luminal surface. Opened stents were fixed with 2% glutaraldehyde in sodium cacodylate buffer with 0.1 M sodium chloride and then rinsed, dehydrated with serial ethanol dilutions followed by hexamethyldisi-lazane (HMDS, EMS), and sputter-coated with gold palladium (Polaron, Williston, VT) as described previously [27]. Ten digital micrographs at random areas were recorded for analysis using SEM (Quanta250, FEI, Hillsboro, OR).

1.10. Tissue Processing and morphometric analyses

Explanted stented arterial segments were fixed in 4% formaldehyde for 48 hours followed by incubation in a mixture of nitric and hydrofluoric acids (1.5 and 5 N final concentrations, respectively) at 28°C for 4 hours to dissolve stainless steel struts. Removal of metal wires allowed subsequent embedding in paraffin wax and microtome sectioning. Eight to ten 6-micron sections were generated from each artery and stained according to Verhoef-van Gieson elastic stain protocol. The arterial micrographs were captured as digital images under 40x magnification, and the areas of lumen, neointima and media were calculated using Image J -generated tracings of the respective anatomic compartments. The extent of ISR expressed as the neointima/media ratio and the percent of cross-sectional stenosis was determined for each section using computerized morphometry. The raw data was averaged for each animal and was further used for statistical comparison between groups.

1.11. Immunofluorescence

4% formaldehyde-fixed stented arteries were exposed to 1.5N nitric/5 N hydrofluoric acid at 28°C for 3 hours to dissolve stainless steel wires and the “destented” arteries were routinely paraffin-embedded and cut into 8-micron sections. After deparaffinization, pH 9-buffer thermal epitope retrieval and blocking in 10% horse serum, the sections were consecutively exposed to mouse anti-rat CD62P antibody (LifeSpan BioSciences) or mouse anti rat-CD68 antibody (Serotec), horse anti-mouse biotinylated secondary antibody (Vector Labs) and DyLight548-labeled streptavidin (Vector Labs), and imaged to visualize platelet deposition and macrophage infiltration of stent-implanted arteries, respectively. The number of CD68-positive cells associated with tissue defects left behind by the dissolved stent struts was used as an index for macrophage infiltration. A fraction of the strut defect circumference exhibiting continuous CD62P staining pattern was employed as an index of platelet deposition on stents. The immunofluorescence data was obtained from 3-5 sections per artery and were further used without averaging for statistical analysis.

1.12. Statistical Analysis

Data were calculated as means ± standard deviation. Statistical analysis of the difference between groups was assessed using analysis of variance (ANOVA), followed by Tukey's test. Statistical significance was noted where $p \leq 0.05$.

2. Results

2.1. Functionalization of Steel Surfaces with CD47

The chemical modification scheme illustrated in Figure 1, was used to functionalize steel surfaces with recCD47 and pepCD47. The quantification assay based on tagging CD47 with biotin, with subsequent use of avidin/peroxidase-containing ABC reagent, and colorimetric peroxidase detection was developed. The amount of CD47 on the surfaces was determined by comparison to a standard curve of recCD47 treated in the same manner. As shown in Figure 2 A, there were 164±30.2 ng/cm^2 and 114.5±28.1 ng/cm^2 on the recCD47 and pepCD47 modified steel surfaces respectively. In contrast, the measured levels on unmodified surfaces or BSA modified control surfaces were negligible.

To investigate the role of passive adsorption of CD47 versus stable covalent attachment to the steel surface, recCD47 immobilization efficiency was compared in the samples treated according to the established conjugation protocol or to a modified protocol omitting the steps of PEI-PDT reduction and sulfo-LC-SPDP modification. The absence of the grafting cross-linker (sulfo-LC-SPDP) significantly reduced the immobilization density of CD47 (from 137±12.3 to 19.2±1.4 ng/cm^2) thus indicating that a non-specific adsorption of CD47 accounts for ~14% of total binding (Fig. 2 B).

2.2. In vitro anti-Inflammatory capacity of CD47-functionalized steel surfaces

To assess the *in vitro* anti-inflammatory capacity of CD47-functionalization, steel foils were modified with CD47 and assessed for their ability to inhibit monocyte-derived macrophage THP-1 cell attachment compared to unmodified foils and control foils (Figure 3). Both recCD47 (62.95±24.48 adhered cells) and pepCD47 (49.52±16.64) significantly ($p \leq 0.0001$) reduced cell attachment compared to unmodified (90.85±12.78), scrambled control peptide (97.04±29.70), and BSA-modified (103.07±17.64) steel foils, indicating that CD47 can inhibit acute inflammation by inhibiting inflammatory cell attachment to steel surfaces.

2.3. Chandler Loop ex vivo model

We used the Chandler Loop Apparatus to better assess the blood interactions with CD47-modified metallic surfaces. Briefly, fresh whole human or rat blood was perfused through polymeric tubing with steel inserts inserted into the tubing. After three hours, the steel tube inserts were removed and processed as detailed above to assess cell adhesion to the unmodified and control surfaces. As shown in Figure 4, immobilized recCD47 (5.15±4.62 adhered cells) and pepCD47 (8.33±6.17) significantly inhibited inflammatory cell attachment to the steel inserts compared to unmodified (113.78±38.88), scrambled peptide (72.70±12.62), or BSA-modified (46.04±12.59) inserts. The *ex vivo* rat blood data suggest that recCD47 (36.53±15.75), pepCD47 (20.50±10.66), and thiol-pepCD47 (21.83±11.31) all significantly inhibit inflammatory cell attachment to the steel inserts compared to unmodified (106.03±27.17), scrambled peptide (82.17±33.60), or BSA-modified (83.67±6.28.07) inserts (Figure 5). Of the three CD47 variants used, the thiol-pepCD47 utilizes the most direct chemical modification that did not appear to inhibit the anti-inflammatory capacity of CD47. Thus we utilized the thiol-pepCD47 in the *in vivo* rat studies.

2.4. Endothelium formation on functionalized steel surfaces

The ability of a vascular stent modification to allow the formation of a healthy endothelial layer is an important step in establishing the anti-inflammation nature of the vascular wall. To that end we examined the affinity of cultured endothelial cells on CD47-modified and control metallic surfaces under physiologically relevant conditions. HUVECs were cultured to confluency on unmodified, recCD47, pepCD47, and BSA-modified steel foils and were exposed to 25 dynes/cm^2 shear stress for 4 hr. After 4 hr of shear stress, all steel samples exhibited minimal cell loss and healthy HUVEC morphology, suggesting that CD47 does not inhibit endothelial cell growth and retention during shear stress (Figure 6a and b). Of note, the cellular morphology observed from the acquired images seemed to suggest that HUVECs cultured on recCD47 and pepCD47-modified steel exhibit a qualitatively greater elongation in the direction of shear stress indicating a level of possible mechanotransduction with this set of conditions.

2.5. In vivo efficacy of CD47-functionalized stents

We assessed the ability of CD47 to prevent acute and chronic inflammatory responses *in vivo* by placing vascular stents into rat carotid arteries as previously described [28]. The stents were removed after 30 min, 3 days, and 14 days to assess acute thrombosis, the inflammatory response, stent-induced neointimal hyperplasia, respectively. Qualitative SEM analysis of explanted stents following 30 min after stent deployment, showed wide-scale fibrin deposition with entrapped red cells, white cells and platelets on the bare metal stent surfaces. These findings are indicative of a strong acute inflammatory and thrombotic response, which is dramatically reduced in the thiol-pepCD47-functionalized stent that demonstrates what appear to be a relatively low amount of platelets that do not exhibit spreading (Figure 7, right panel). The qualitative SEM findings are further corroborated with the quantitative assay based on immunofluorescent staining that demonstrated a 36% reduction of platelet accumulation on the struts (Figure 9, upper panel). These platelet results are consistent with our previous data obtained from CD47-functionalized polymers [14]. To assess the anti-restenosis efficacy of CD47-functionalization, the stents were removed after 14 days in a separate group of rats. As shown in Figure 8, restenosis measures, both stenosis and neointimal hyperplasia, were significantly reduced, demonstrating that CD47-functionalization mitigates ISR.

The inflammatory response to implanted cardiovascular devices is characterized by a temporal change in the cellular profile at the interface between the host tissue and the biomaterial surface. We used immunofluorescence to obtain qualitative and quantitative data regarding the changes in the inflammatory cell type at the stent struts as a function of CD47 modification. The stent-associated cells identified were platelets and macrophages at the respective time points: 30 min and 3 days. Our data suggest that CD47 significantly reduces both platelet attachment to the stent struts at 30 min and macrophage recruitment after 3 days (Figure 9). Overall, these experiments demonstrate the ability of CD47 to specifically inhibit the cell types involved in the inflammatory response. Taken together, these results suggest that CD47 functionalization of vascular stents may prove to be an effective strategy for preventing inflammation and restenosis associated with stent deployment.

3. Discussion

Although endovascular stents are widely used, their long-term effectiveness is limited by ISR. We present herein early feasibility studies that show the effectiveness of a bioactive surface coating in which recombinant CD47, or a relevant peptide sequence thereof, are immobilized onto steel surfaces with the overarching goal of inhibiting early stage pro-inflammatory events that contribute to ISR. To that end, this work represents the first *in vivo* demonstration of the use of immobilized CD47 in a functioning medical device. We also expand upon the current understanding of CD47 physiology as it pertains to the molecule's structure and function as well as the role of CD47 upon platelet physiology. Together these data strongly suggest that immobilized CD47 can be an effective therapeutic strategy in addressing ISR.

Low-grade inflammation has been established as a hallmark of vasculo-proliferative diseases, such as ISR. Vascular intervention, a precipitating event for ISR, consistently triggers inflammatory reaction that traverses through the acute and chronic phases with a typical sequence of blood-borne cell recruitment, activation, and loss via apoptotic death or emigration (efferocytosis). Previous work in the field has demonstrated a therapeutic value of strategies based on systemic or local attenuation of neutrophils [10, 29] and macrophages [30, 31], the main cell types mediating acute and chronic phases of inflammatory response, respectively. Additionally, elevated platelet count and function are also recognized ISR risk factors [32, 33]. A non-occluding thrombus formed over the stent struts immediately after stent implantation serves as a nidus for SMC migrating from the media in response to gradient of platelet-secreted growth factors, mainly PDGF BB. Moreover, platelet deposits facilitate leukocyte attachment to the injured artery through direct β2-integrin (Mac-1) binding to platelet glycoprotein GP1bα [34]. The role of platelets in ISR pathology is further corroborated by the fact that thrombocytopenia reduces neointimal volume in rat [35] and rabbit models [36]. In our studies, functionalization of stent surface with CD47 reduced both early attachment of platelets at 30 min after stenting and macrophage recruitment to the stent/artery interface at 3 days after stent deployment. Importantly, this was achieved locally without systemically affecting platelet and monocyte numbers and function, thus obviating hemorrhagic and infectious risks inherent to generalized attenuation of these cell types.

In addition to SIRPα, thrombosponin-1 (TSP-1) is a known ligand of CD47. The deleterious role of TSP-1 in vascular response to injury is well established [37, 38]. It is noteworthy that beyond direct upregulation of TSP-1 expression due to vascular trauma, metal ions released from the stent surface can sustain high TSP-1 production for prolonged time [39]. Although not addressed by our present studies, it is feasible that the decrease of TSP-1 in vascular tissue due to sequestering of TSP-1 by CD47-derivatized stents plays an auxiliary role in the antirestenotic effect of CD47 functionalization of stent surface.

In our therapeutic experiment, implantation of CD47-modified stents was associated with less severe ISR compared to BMS. In this pilot study, we used a single loading of CD47. To that end, we noted approximately a 25% reduction in neointimal formation. These results are modest and may be related to a number of factors including the use of a non-optimized CD47 dose, the residual inflammatory cell burden (Fig. 9) or to the concurrent ISR mechanisms, such as direct SMC-activating effects of vascular trauma that are not immediately related to vascular inflammation. Different pathogenic mechanisms are implicated in the neointimal growth at the different times after vascular injury. It is feasible that surface immobilized pepCD47 provides less or no protection against delayed events, such as proliferation of neointimal SMC and ECM synthesis, while significantly blocking early medial SMC proliferation and migration that are directly triggered by the upsurge of inflammatory cytokines.

We have previously shown that the immobilization strategy used to append CD47 to polymeric surfaces is readily dose-adjustable [16]. Specifically, we demonstrated that concentrations of CD47 over 100 ng/cm^2 significantly inhibited inflammatory cell attachment and chose 250 ng/cm^2 as a working concentration for the subsequent experiments [16]. The immobilization chemistry, demonstrated herein, used to functionalize metallic surfaces with CD47 can also be adjusted. In these initial studies we used a surface concentration (~160 ng/cm^2) between the effective values derived from the polymer studies. Where the *in vitro* and *ex vivo* experiments performed in these studies, and the previous studies of CD47 on polymeric surfaces [16], showed almost complete inhibition of cell attachment. The results of the *in vivo* studies in the experiments presented herein did not demonstrate a total reduction in inflammatory cell attachment. This difference can be likely explained by the limitations of applying *in vitro* and *ex vivo* observations into *in vivo* systems in such complicated pathophysiological processes as ISR. The pharmacological potential of CD47 immobilized stents has not been fully explored and future studies will address a dose-effect relationship between the CD47 immobilization density and the anti-restenotic effect to identify the most appropriate CD47 loading on stent, resulting in maximal ISR inhibition. Based upon the results presented, such dose-response studies will necessitate the use of short-term *in vivo* models that were beyond the scope of the current investigations. With respect to future investigations, considering translational potential of CD47 functionalized stents, comparison of CD47 stents with current gold standard DES is paramount. Unfortunately, no DES products are available in the size fitting rat arteries, therefore this comparison will be conducted in rabbit model at the next phase of our program.

Numerous research efforts have been directed towards the development and optimization of DES, which have demonstrated a measurable reduction in ISR. However DES are limited in many aspects, including off-target drug effects, a finite amount of drug capacity, issues with release time, and the cost to manufacture [40, 41]. In addition, stent thrombosis remains a serious concern for both DES and bare metal stents [2, 3]. In the case of DES, the polymeric coating that functions as the drug delivery platform elicits an inflammatory response, and drugs contained in DES such as paclitaxel can inhibit reendothelialization and thereby contribute to late stage stent thrombosis [5]. Given these limitations of DES, we decided to utilize an immunomodulatory system that we have previously shown was successful with implantable polymers.

Compared to DES, the use of immobilized CD47 on the surface of metallic stents does not require a polymeric coating and CD47 can inhibit inflammatory cell activation [14, 16, 42, 43]. There is also a growing body of evidence from our laboratory that CD47 can inhibit platelet activation and attachment. These previous results are supported by our in vivo results, presented herein, which show a stark reduction in fibrin deposition and platelet attachment (Figures 7 and 9). As addressing late stent thrombosis after implantation remains an unmet need in interventional cardiology[44, 45], our findings suggest a potential therapeutic application (re. reducing platelet deposition) for immobilized CD47 on the stent surface. In addition, our initial *in vitro* assessment indicated that modifying the metallic surfaces with CD47 did not appear to inhibit endothelial cell attachment or retention following exposure to physiologically relevant levels of laminar shear stress. These results are consistent with our previous studies investigating the mechanistic role of CD47 in outgrowth endothelial cell attachment and retention of lipid modified polymers [46]. Although a direct comparison between DES and CD47 modified stents was not undertaken in these initial studies, it must be noted that we have extensively characterized the use of CD47 on polymeric surfaces. With respect to long-term applications of immobilized polymeric CD47 surfaces, in a 7-week rat subdermal implant study, we demonstrated that CD47 was retained and remained effective in preventing inflammatory cell mediated oxidative damage to the polyurethane films [16]. Therefore, appending CD47 to the surface of DES as an anti-inflammatory and anti-thrombotic supplement to the anti-ISR of the DES would hypothetically be feasible and provide a durable anti-inflammatory stent surface.

SIRPα is a member of the immunoreceptor tyrosine-based inhibitory motif (ITIM) containing family which is responsible for modulating the immune response (reviewed in [43]). Targeting SIRPα signaling pathways, via immobilizing CD47 to the stent surface, represents a bioactive strategy to address the issue of ISR. Work by others has shown that appending bioactive molecules, such as heparin and tropoelastin, to endovascular stents has improved the devices' biocompatibility [47, 48]. Thus, specifically targeting key molecular signaling pathways may represent a new direction in addressing the biocompatibility issues associated when large volumes of blood are perfused over the synthetic surfaces that constitute the biointerface of cardiovascular devices.

The anti-inflammatory and anti-thrombotic capacity of the CD47 and SIRPα signaling pathway has not been fully characterized. Our previous work with polymeric biomaterials, such as polyurethane and polyvinyl chloride (PVC), has shown that CD47-functionalization prevents inflammatory cell attachment and activation as well as decreases the foreign body response in a rat subdermal implant model [14, 16, 42]. In addition, we demonstrated that platelets express SIRPα and are responsive to immobilized CD47 on the surface of PVC. These previous studies used recombinant CD47 as the effector molecule on the polymeric surfaces. Where recombinant proteins may be useful for such relatively small surfaces as endovascular stents, their application on larger surfaces presents an economical and technical challenge.

Our use of the pepCD47 was motivated by a previous report demonstrating that the peptide sequence was sufficient to prevent the phagocytosis of opsonized nanobeads through its association with SIRPα [18]. Interestingly, additional investigations suggested that the CD47 peptide does not bind to SIRPα [49]. However, this more recent paper did not address the biological activity noted by the first group. Through the use of relevant controls, namely the scrambled peptide sequence, and multiple experimental systems, our biological results strongly suggest that pepCD47 associates with SIRPα to facilitate the downstream events. Our results, detailed in this work, indicated that the CD47 peptide exhibits similar properties as the recombinant CD47 protein that has been established to be mediated through its interaction with SIRPα [14, 16, 42, 43].

Peptides tend to be more readily modifiable than recombinant proteins, which we have demonstrated using both lysine-modified and cysteine-modified (thiol-CD47) versions of the CD47 peptide. The thiol-pepCD47 is synthesized to contain a thiol-reactive cysteine residue on the C-terminal end allowing for more direct modification chemistry by eliminating the need for SPDP conjugation to pepCD47, because the thiol-reactive cysteine residues react directly with the thiol-reactive PDT groups installed through PEI-PDT modification. This allowed us to modify the attachment chemistry to eliminate avoidable steps and start to streamline production. However, the use of peptides presents technical challenges. They can be much harder to identify unless they are tagged in some manner or an antibody exists for their detection. These limitations were addressed by developing a new quantification methodology based on biotinylating the CD47 (rec and pep variants) prior to appendage to the steel. Once biotinylated, the chemistry described in Figure 1 was followed and the avidin/biotinylated peroxidase-containing ABC reagent was used to detect the biotinylated CD47 attached to the model steel surface. The amount of surface-immobilized peroxidase (as a proxy to the amount of CD47) was quantified colorimetrically against the calibration curve constructed with the known amounts of biotinylated antibody, using TMB substrate allowing for the development of a detectable color product in solution, as shown in Figure 2. The data collected from this quantification assay provided similar immobilization densities to our previous data from polymers [14, 16, 42, 43]. Therefore, this modification procedure provides a highly reproducible and quantifiable method of appending CD47 to steel surfaces.

4. Conclusions

These experiments demonstrated the efficacy of the use of immobilized CD47 in inhibiting early inflammatory and thrombotic events that contribute to the pathophysiology of arterial injury post-stent angioplasty. Specifically we show stent surfaces can be modified with either recombinant CD47 or peptide derived from CD47 Ig domain. We also demonstrated, using *in vitro* and *in vivo* model systems, immunomodulatory activity and platelet inhibition with CD47 modified metal surfaces. In addition, our results show that CD47 modified stents induce significantly less restenosis than unmodified stents.

Acknowledgements

Support for JBS from NIH T32 HL007915. Support for SJS, IF, and IA from NIH R21 EB015612. Additional support for IA was from NIH R01 HL72108. Support for RJL from the William J. Rashkind Endowment, Erin's Fund of the Children's Hospital of Philadelphia and The Kibel Foundation. Support for CN and JWW from NIH HL090774. The angioplasty catheters used in animal experiments were kindly donated by NuMed (Hopkinton, NY). Support for scanning electron microscope from S10 OD018041. The CD47 technology is licensed to SIRP Biological Coatings Inc. of which RJL and SJS are co-founders and equity shareholders. The authors would like to acknowledge Sy-Dar Liou and Jamie Cohen for their technical assistance.

References

1. Mozaffarian D, Benjamin EJ, Go AS, Arnett DK, Blaha MJ, Cushman M, et al. Heart disease and stroke statistics--2015 update: a report from the American Heart Association. Circulation. 2015; 131:e29–322. [PubMed: 25520374]
2. Butt M, Connolly D, Lip GY. Drug-eluting stents: a comprehensive appraisal. Future cardiology. 2009; 5:141–57. [PubMed: 19371189]
3. Simard T, Hibbert B, Ramirez FD, Froeschl M, Chen YX, O'Brien ER. The evolution of coronary stents: a brief review. Can J Cardiol. 2014; 30:35–45. [PubMed: 24286961]
4. Rathore S, Terashima M, Katoh O, Matsuo H, Tanaka N, Kinoshita Y, et al. Predictors of angiographic restenosis after drug eluting stents in the coronary arteries: contemporary practice in real world patients. EuroIntervention. 2009; 5:349–54. [PubMed: 19736160]
5. Jaffe R, Strauss BH. Late and very late thrombosis of drug-eluting stents: evolving concepts and perspectives. J Am Coll Cardiol. 2007; 50:119–27. [PubMed: 17616295]
6. Clark MA, Bakhai A, Lacey MJ, Pelletier EM, Cohen DJ. Clinical and economic outcomes of percutaneous coronary interventions in the elderly: an analysis of medicare claims data. Circulation. 2004; 110:259–64. [PubMed: 15226211]
7. Mitra AK, Del Core MG, Agrawal DK. Cells, cytokines and cellular immunity in the pathogenesis of fibroproliferative vasculopathies. Canadian journal of physiology and pharmacology. 2005; 83:701–15. [PubMed: 16333372]
8. Ramji DP, Davies TS. Cytokines in atherosclerosis: Key players in all stages of disease and promising therapeutic targets. Cytokine Growth Factor Rev. 2015
9. Toutouzas K, Karanasos A, Stefanadis C. Inflammatory mechanisms of adverse reactions to BMS. Curr Vasc Pharmacol. 2013; 11:379–91. [PubMed: 23905633]
10. Welt FG, Rogers C. Inflammation and restenosis in the stent era. Arterioscler Thromb Vasc Biol. 2002; 22:1769–76. [PubMed: 12426203]
11. Billinger M, Buddeberg F, Hubbell JA, Elbert DL, Schaffner T, Mettler D, et al. Polymer stent coating for prevention of neointimal hyperplasia. J Invasive Cardiol. 2006; 18:423–6. discussion 7. [PubMed: 16954581]
12. Menown I, Lowe R, Penn I. Passive stent coatings in the drug-eluting era. J Invasive Cardiol. 2005; 17:222–8. [PubMed: 15831978]
13. Windecker S, Mayer I, De Pasquale G, Maier W, Dirsch O, De Groot P, et al. Stent coating with titanium-nitride-oxide for reduction of neointimal hyperplasia. Circulation. 2001; 104:928–33. [PubMed: 11514381]
14. Finley MJ, Rauova L, Alferiev IS, Weisel JW, Levy RJ, Stachelek SJ. Diminished adhesion and activation of platelets and neutrophils with CD47 functionalized blood contacting surfaces. Biomaterials. 2012; 33:5803–11. [PubMed: 22613135]
15. Slee JB, Alferiev IS, Levy RJ, Stachelek SJ. The use of the ex vivo Chandler Loop Apparatus to assess the biocompatibility of modified polymeric blood conduits. J Vis Exp. 2014
16. Stachelek SJ, Finley MJ, Alferiev IS, Wang F, Tsai RK, Eckells EC, et al. The effect of CD47 modified polymer surfaces on inflammatory cell attachment and activation. Biomaterials. 2011; 32:4317–26. [PubMed: 21429575]
17. West JL, Hubbell JA. Separation of the arterial wall from blood contact using hydrogel barriers reduces intimal thickening after balloon injury in the rat: the roles of medial and luminal factors in arterial healing. Proc Natl Acad Sci U S A. 1996; 93:13188–93. [PubMed: 8917566]
18. Rodriguez PL, Harada T, Christian DA, Pantano DA, Tsai RK, Discher DE. Minimal “Self” peptides that inhibit phagocytic clearance and enhance delivery of nanoparticles. Science. 2013; 339:971–5. [PubMed: 23430657]
19. Lee CK, Koo KT, Park YJ, Lee JY, Rhee SH, Ku Y, et al. Biomimetic surface modification using synthetic oligopeptides for enhanced guided bone regeneration in beagles. J Periodontol. 2012; 83:101–10. [PubMed: 21542731]
20. Lee JY, Choi YS, Lee SJ, Chung CP, Park YJ. Bioactive peptide-modified biomaterials for bone regeneration. Curr Pharm Des. 2011; 17:2663–76. [PubMed: 21728982]

21. Sreejalekshmi KG, Nair PD. Biomimeticity in tissue engineering scaffolds through synthetic peptide modifications-altering chemistry for enhanced biological response. J Biomed Mater Res A. 2011; 96:477–91. [PubMed: 21171167]
22. Fishbein I, Alferiev I, Bakay M, Stachelek SJ, Sobolewski P, Lai M, et al. Local delivery of gene vectors from bare-metal stents by use of a biodegradable synthetic complex inhibits in-stent restenosis in rat carotid arteries. Circulation. 2008; 117:2096–103. [PubMed: 18413497]
23. Fishbein I, Alferiev IS, Nyanguile O, Gaster R, Vohs JM, Wong GS, et al. Bisphosphonate-mediated gene vector delivery from the metal surfaces of stents. Proc Natl Acad Sci U S A. 2006; 103:159–64. [PubMed: 16371477]
24. Hermanson, GT. Bioconjugation Techniques. Third ed. Academic Press; 2013. The reactions of bioconjugation.; p. 229-58.Chapter 3
25. Fishbein I, Forbes SP, Chorny M, Connolly JM, Adamo RF, Corrales RA, et al. Adenoviral vector tethering to metal surfaces via hydrolyzable cross-linkers for the modulation of vector release and transduction. Biomaterials. 2013; 34:6938–48. [PubMed: 23777912]
26. Stachelek SJ, Alferiev I, Connolly JM, Sacks M, Hebbel RP, Bianco R, et al. Cholesterol-modified polyurethane valve cusps demonstrate blood outgrowth endothelial cell adhesion post-seeding in vitro and in vivo. Ann Thorac Surg. 2006; 81:47–55. [PubMed: 16368333]
27. Vorjohann S, Fish RJ, Biron-Andreani C, Nagaswami C, Weisel JW, Boulot P, et al. Hypodysfibrinogenaemia due to production of mutant fibrinogen alpha-chains lacking fibrinopeptide A and polymerisation knob 'A'. Thromb Haemost. 2010; 104:990–7. [PubMed: 20806111]
28. Fishbein I, Forbes SP, Adamo RF, Chorny M, Levy RJ, Alferiev IS. Vascular gene transfer from metallic stent surfaces using adenoviral vectors tethered through hydrolysable cross-linkers. J Vis Exp. 2014:e51653. [PubMed: 25145470]
29. Wang Y, Sakuma M, Chen Z, Ustinov V, Shi C, Croce K, et al. Leukocyte engagement of platelet glycoprotein Ibalpha via the integrin Mac-1 is critical for the biological response to vascular injury. Circulation. 2005; 112:2993–3000. [PubMed: 16260637]
30. Danenberg HD, Fishbein I, Epstein H, Waltenberger J, Moerman E, Monkkonen J, et al. Systemic depletion of macrophages by liposomal bisphosphonates reduces neointimal formation following balloon-injury in the rat carotid artery. J Cardiovasc Pharmacol. 2003; 42:671–9. [PubMed: 14576517]
31. Danenberg HD, Fishbein I, Gao J, Monkkonen J, Reich R, Gati I, et al. Macrophage depletion by clodronate-containing liposomes reduces neointimal formation after balloon injury in rats and rabbits. Circulation. 2002; 106:599–605. [PubMed: 12147543]
32. Jaster M, Horstkotte D, Willich T, Stellbaum C, Knie W, Spencker S, et al. The amount of fibrinogen-positive platelets predicts the occurrence of in-stent restenosis. Atherosclerosis. 2008; 197:190–6. Epub 2007 May 7. [PubMed: 17485094]
33. Norgaz T, Hobikoglu G, Aksu H, Bolca O, Uyarel H, Eren M, et al. The relationship between preprocedural platelet size and subsequent in-stent restenosis. Acta Cardiol. 2004; 59:391–5. [PubMed: 15368800]
34. Simon DI, Chen Z, Xu H, Li CQ, Dong J, McIntire LV, et al. Platelet glycoprotein ibalpha is a counterreceptor for the leukocyte integrin Mac-1 (CD11b/CD18). J Exp Med. 2000; 192:193–204. [PubMed: 10899906]
35. Fingerle J, Johnson R, Clowes AW, Majesky MW, Reidy MA. Role of platelets in smooth muscle cell proliferation and migration after vascular injury in rat carotid artery. Proc Natl Acad Sci U S A. 1989; 86:8412–6. [PubMed: 2813399]
36. Friedman RJ, Stemerman MB, Wenz B, Moore S, Gauldie J, Gent M, et al. The effect of thrombocytopenia on experimental arteriosclerotic lesion formation in rabbits. Smooth muscle cell proliferation and re-endothelialization. J Clin Invest. 1977; 60:1191–201. [PubMed: 409735]
37. Chen D, Asahara T, Krasinski K, Witzenbichler B, Yang J, Magner M, et al. Antibody blockade of thrombospondin accelerates reendothelialization and reduces neointima formation in balloon-injured rat carotid artery. Circulation. 1999; 100:849–54. [PubMed: 10458722]

38. Rittersma SZ, Boekholdt SM, Koch KT, Geuzebroek R, Bax M, Schotborgh CE, et al. Thrombospondin gene polymorphisms and the risk of angiographic coronary in-stent restenosis. Am J Med. 2004; 116:499–500. [PubMed: 15047045]
39. Pallero MA, Talbert Roden M, Chen YF, Anderson PG, Lemons J, Brott BC, et al. Stainless steel ions stimulate increased thrombospondin-1-dependent TGF-beta activation by vascular smooth muscle cells: implications for in-stent restenosis. J Vasc Res. 2010; 47:309–22. [PubMed: 20016205]
40. Lemos PA, Serruys PW, Sousa JE. Drug-eluting stents: cost versus clinical benefit. Circulation. 2003; 107:3003–7. [PubMed: 12821586]
41. Puranik AS, Dawson ER, Peppas NA. Recent advances in drug eluting stents. International journal of pharmaceutics. 2013; 441:665–79. [PubMed: 23117022]
42. Finley MJ, Clark KA, Alferiev IS, Levy RJ, Stachelek SJ. Intracellular signaling mechanisms associated with CD47 modified surfaces. Biomaterials. 2013; 34:8640–9. [PubMed: 23948164]
43. Slee JB, Christian AJ, Levy RJ, Stachelek SJ. Addressing the Inflammatory Response to Clinically Relevant Polymers by Manipulating the Host Response Using ITIM Domain-Containing Receptors. Polymers. 2014; 6:2526–51. [PubMed: 25705515]
44. Byrne RA. Bioresorbable Vascular Scaffolds - Will Promise Become Reality? N Engl J Med. Oct 19.2015
45. Ellis SG, Kereiakes DJ, Metzger DC, Caputo RP, Rizik DG, Teirstein PS, et al. Everolimus-Eluting Bioresorbable Scaffolds for Coronary Artery Disease. N Engl J Med. Oct 12.2015
46. Ueda M, Alferiev IS, Simons SB, Hebbel RP, Levy RJ, Stachelek SJ. CD47-dependent molecular mechanisms of blood outgrowth endothelial cell attachment on cholesterol-modified polyurethane. Biomaterials. 2010; 31:6394–9. [PubMed: 20538335]
47. Krajewski S, Neumann B, Kurz J, Perle N, Avci-Adali M, Cattaneo G, et al. Preclinical evaluation of the thrombogenicity and endothelialization of bare metal and surface-coated neurovascular stents. AJNR American journal of neuroradiology. 2015; 36:133–9. [PubMed: 25258364]
48. Waterhouse A, Yin Y, Wise SG, Bax DV, McKenzie DR, Bilek MM, et al. The immobilization of recombinant human tropoelastin on metals using a plasma-activated coating to improve the biocompatibility of coronary stents. Biomaterials. 2010; 31:8332–40. [PubMed: 20708259]
49. Hatherley D, Lea SM, Johnson S, Barclay AN. Polymorphisms in the human inhibitory signal-regulatory protein alpha do not affect binding to its ligand CD47. J Biol Chem. 2014; 289:10024–8. [PubMed: 24550402]

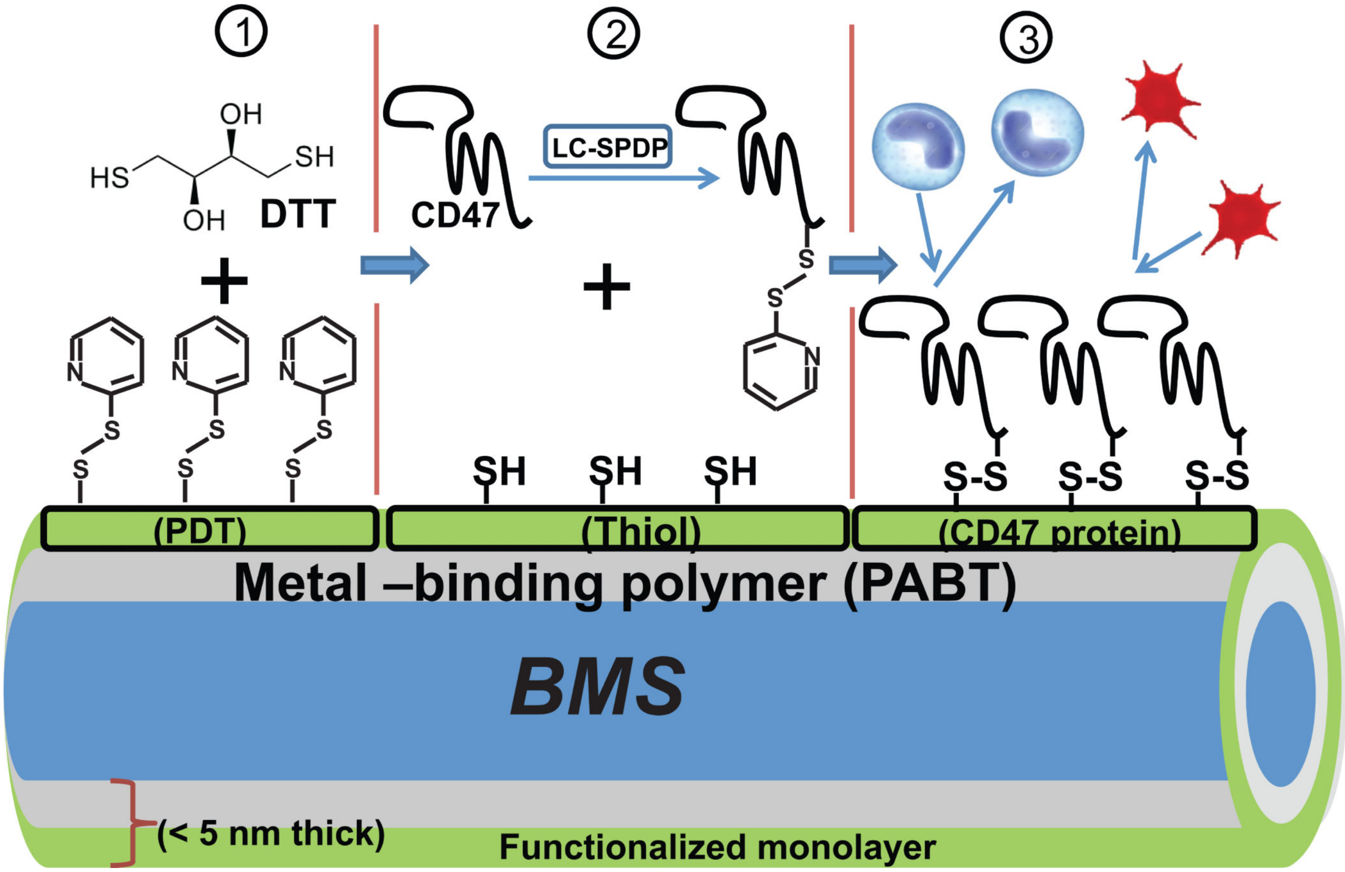

Fig. 1.

Schematic representation of modification chemistry used to append CD47 to bare metal stents (BMS). After modification of steel surfaces with polallylamine bisphosphonate comprising latent thiol groups, PABT and deprotection of latent thiols, the surface was rendered thiol-reactive due to installment of pyridyldithio (PDT) groups using PEI-PDT (step 1). Since only a minor fraction of PDT groups in PEI-PDT is consumed in the reaction with thiols, PEI-PDT acts as an amplifier of thiol groups which are formed during reduction of PDT groups with dithiothreitol, DTT (step 2). In parallel, recCD47 or pepCD47 is modified at poly(Lys) segment with bifunctional (amine-, thiol-reactive) cross-linker, Sulfo-LC-SPDP (step 2). Finally, the thiol-reactive protein moiety is attached via disulfide bridges to the functionalized surface in the course of reaction between surface thiols and protein-bound PDT groups (step 3).

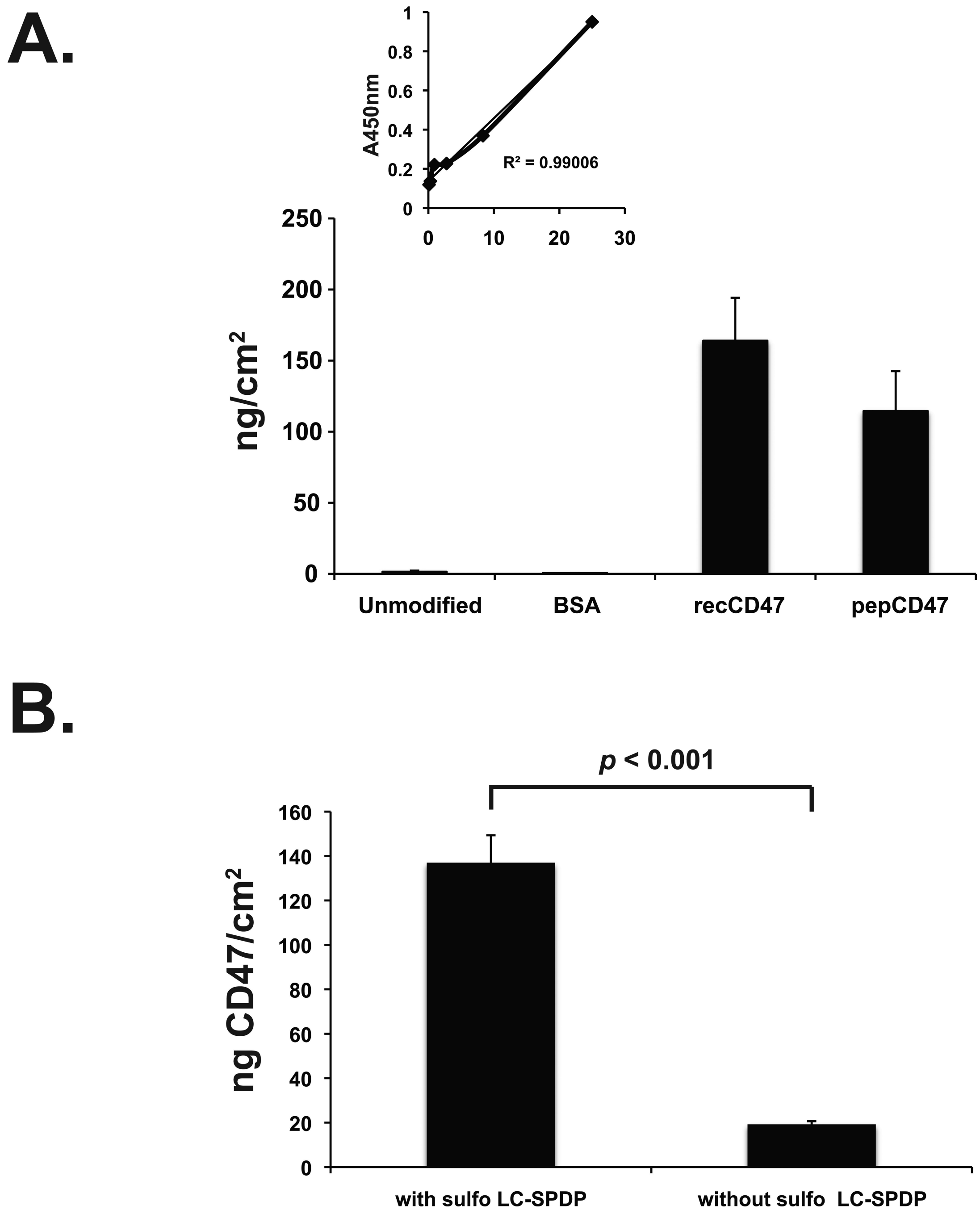

Fig. 2.

CD47 Quantification. (A) The modification chemistry summarized in Figure 1 was utilized to facilitate quantification. Following PEI-PDT addition, primary amines were acetylated using sulfo-NHS-Acetate. recCD47 and pepCD47 were biotinylated using Sulfo-NHS-LC-LC-Biotin. Biotinylated recCD47 and pepCD47 were then reacted with the steel surfaces. ABC reagent and Ultra TMB substrate were used to determine the concentration of CD47 by comparison to a standard curve (inset) prepared using escalating amount of biotinylated IgG

Author Manuscript

Author Manuscript

Author Manuscript

assayed in the same manner. (B) CD47 concentration on steel surfaces in the presence or absence of bi-functional cross-linking agent (sulfo-LC-SPDP).

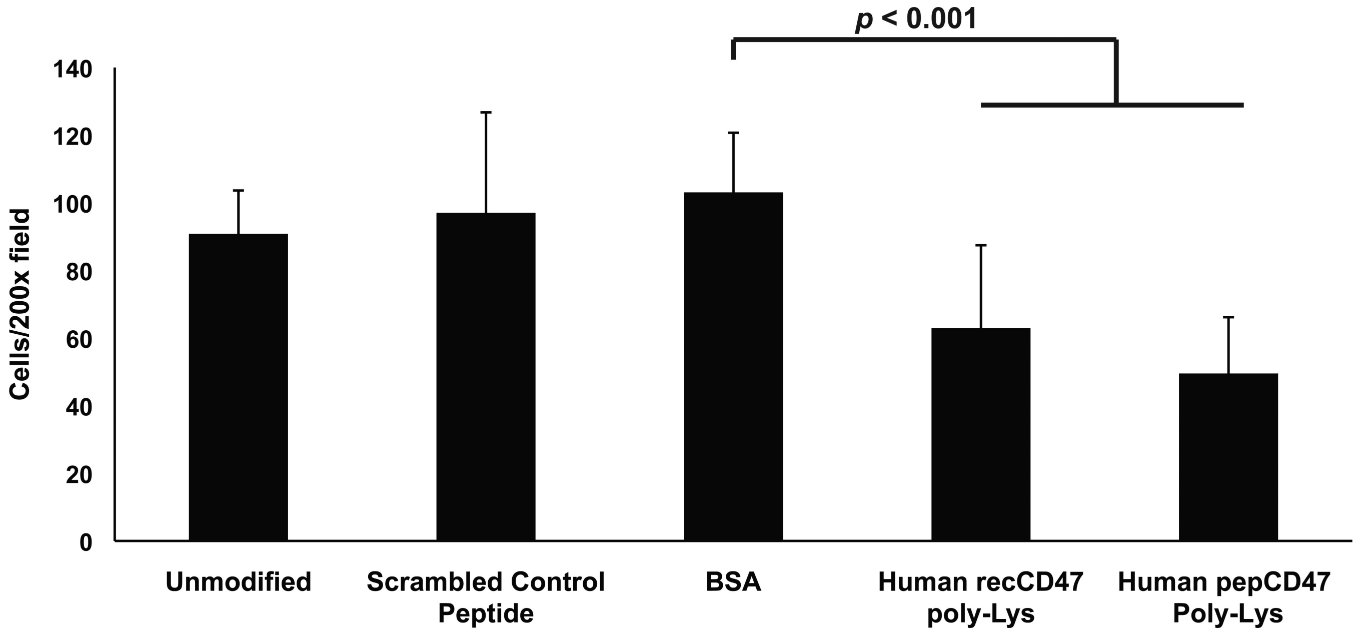

Fig. 3.

CD47 immobilization prevents attachment of cultured monocyte-derived macrophages to steel surfaces. THP-1 cells were differentiated with the addition of PMA to their media and were cultured on steel foils for 3 days. After 3 days, the foils were gently rinsed with DPBS, fixed with 4% formaldehyde, and nuclei stained with DAPI. DAPI staining of adherent cells was visualized and randomly selected 200X fields were counted. Results represent the average and standard deviation of the mean of nine individual fields ($P < 0.0001$).

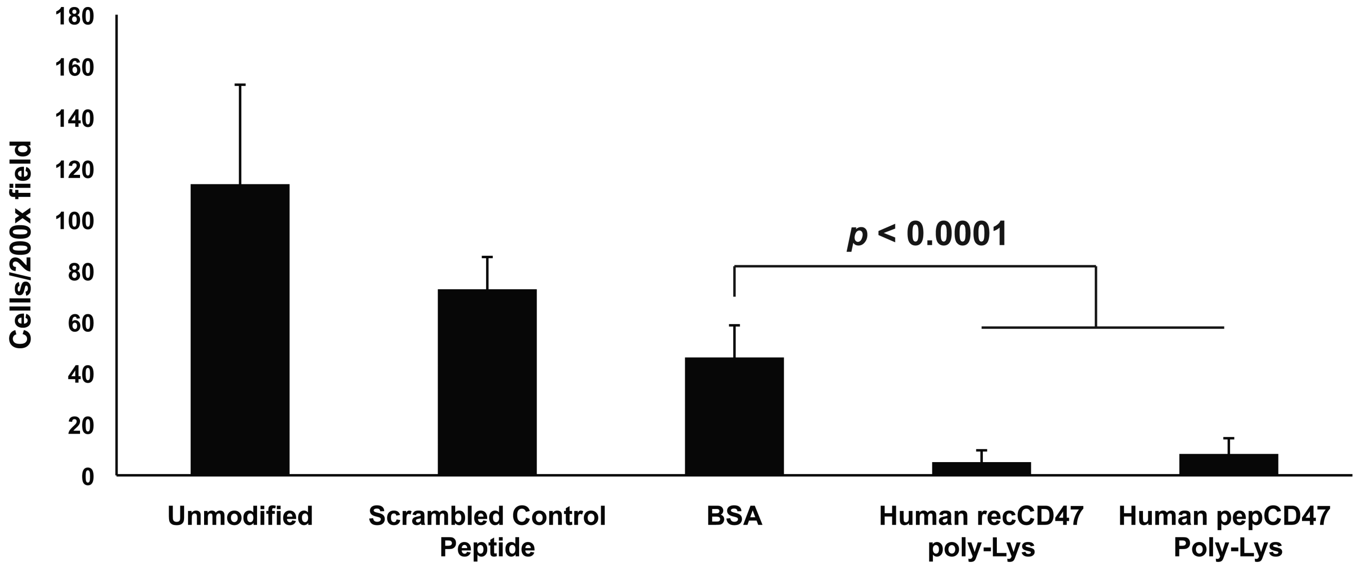

Fig. 4.

CD47 immobilization prevents the attachment of blood leukocytes to stainless steel surfaces. The Chandler Loop apparatus was used, as detailed in *Materials and Methods*, to expose citrate-treated whole human blood to the luminal surface of unmodified steel inserts or BSA, recCD47, or pepCD47-modified steel inserts that were placed into medical grade PVC tube conduits. DAPI staining of adherent cells were visualized, and randomly selected 200X fields were counted. Results show that immobilization of CD47 significantly reduced blood cell adhesion to the steel surfaces. Results represent the average and standard deviation of the mean of nine individual fields ($P < 0.0001$).

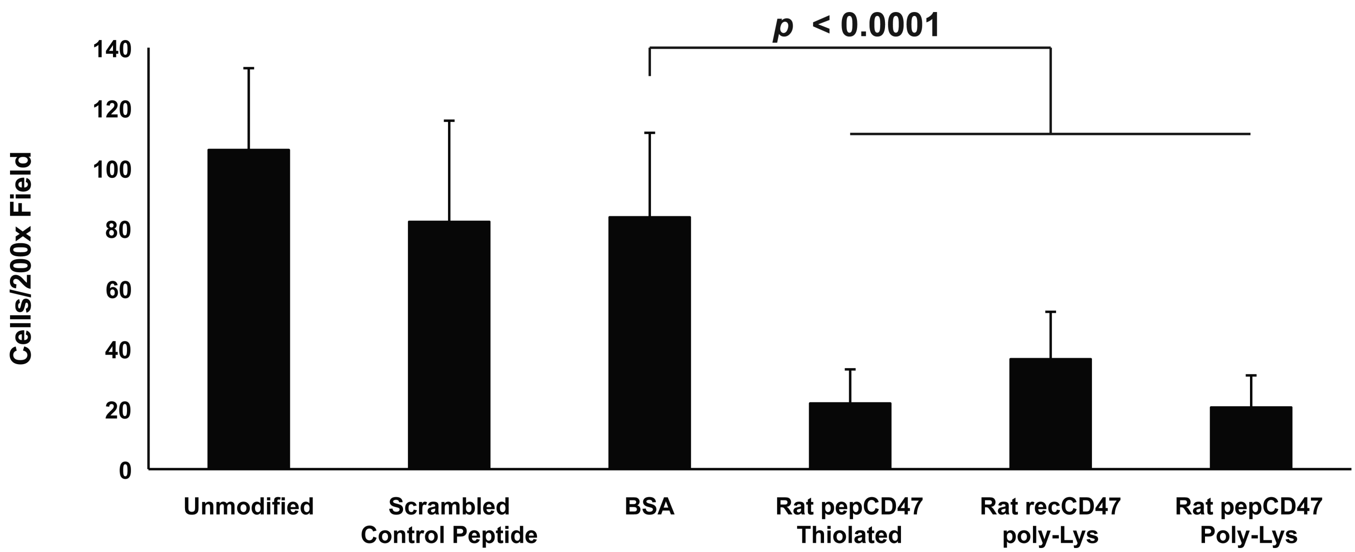

Fig. 5.

Comparative analysis of the effect of rat CD47 immobilization strategy upon blood cell attachment. Thiolated or poly-lysine modified pepCD47, derived from the rat CD47 sequence, were appended to steel inserts as detailed in *Materials and Methods*. Heparinized whole rat blood was perfused, via the Chandler Loop Apparatus, over the luminal surface of unmodified steel inserts or BSA, pepCD47-modified, or recCD47-modified steel inserts, which were placed into medical grade PVC tube conduits. After three hours, the inserts were removed and processed as detailed in *Materials and Methods*. Following DAPI staining, nine randomly selected fields of view under 200X magnification were counted and statistical analyses were performed. Results represent the average and standard deviation of the mean of nine individual fields ($P < 0.0001$).

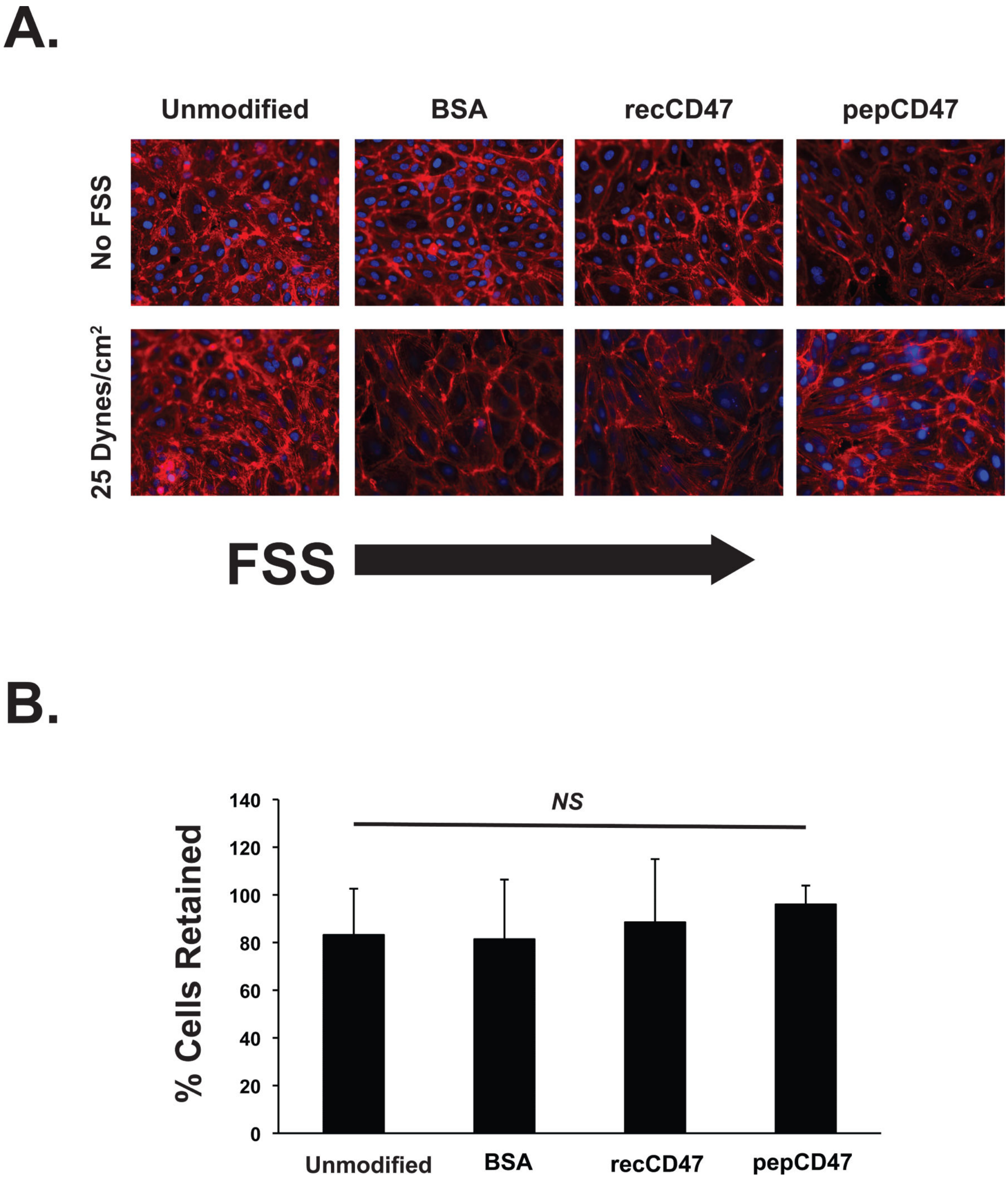

Fig. 6.

Endothelial cell retention, under physiologically relevant shear flow, is not affected by CD47 immobilization. (A) Representative fluorescent micrographs of HUVECs cultured on thiolated pepCD47, recCD47, BSA-modified and unmodified stainless steel surfaces. Once confluent, the HUVECs were exposed to 25 dynes/cm^2 fluid shear stress (FSS) for 4 hr using the FlexCell® Streamer® device. Following shear stress exposure, the HUVECs were fixed and permeabilized. Actin stress fibers were then stained with rhodamine-Phalloidin, following which the nuclei were DAPI stained. (B) DAPI positive cells from nine random fields were counted and compared with cell counts from cultured HUVECs grown on the various surface, but not exposed to FSS. Graph shows percent retention for each surface tested.

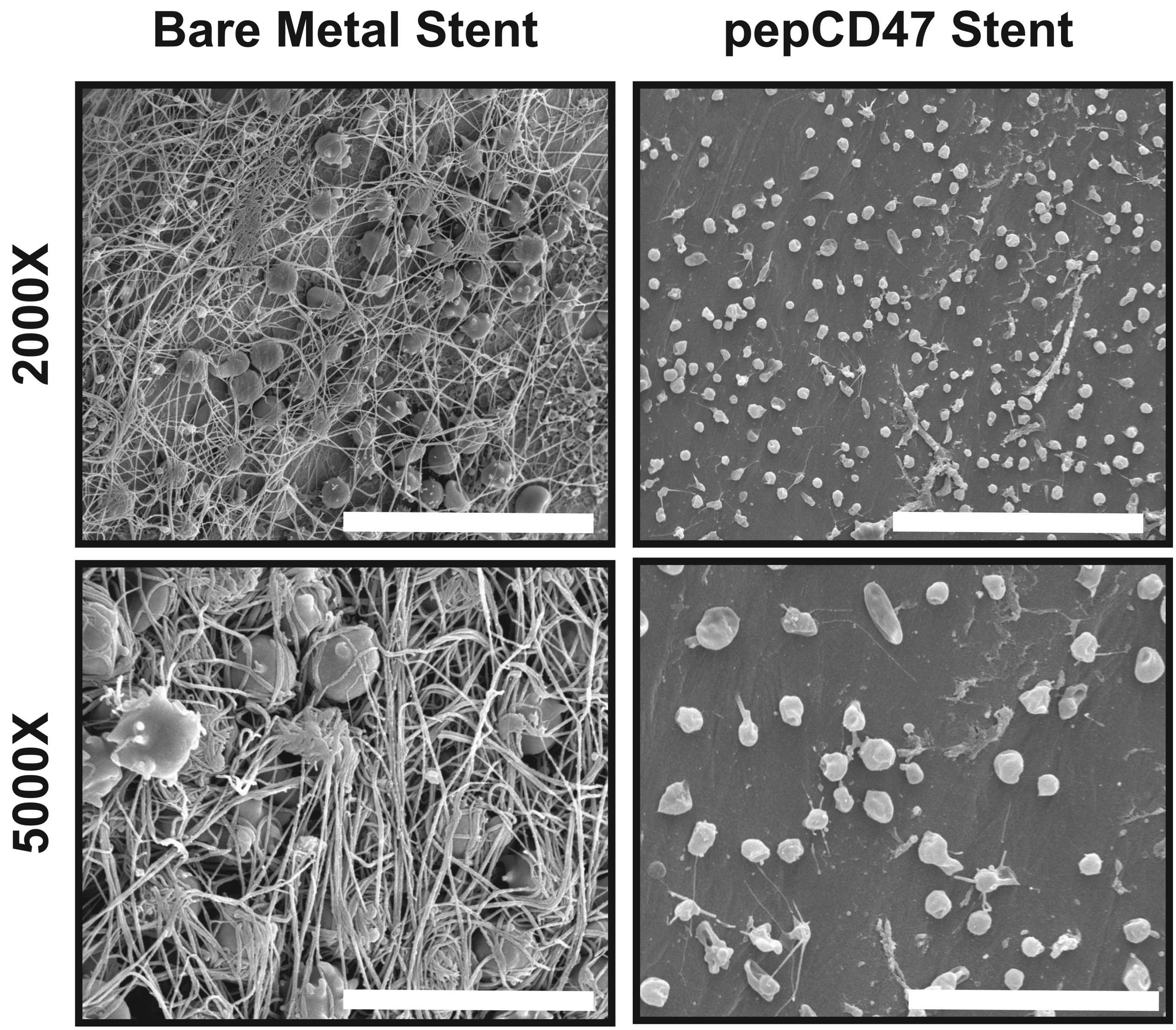

Fig. 7.

Surface characterization of explanted endovascular stent following 30-minute deployment in a rat carotid artery. Representative scanning electron micrographs of the surface of bare metal stents or stents coated with thiolated pepCD47. Images show large fibrin deposition and trapped cells on the unmodified stents surface. In contrast pepCD47 stents exhibited less fibrin on the surface and the attached cells appeared to be more rounded and less spread. Scale Bar = 30 μm (2000X) and 10 μm (5000X)

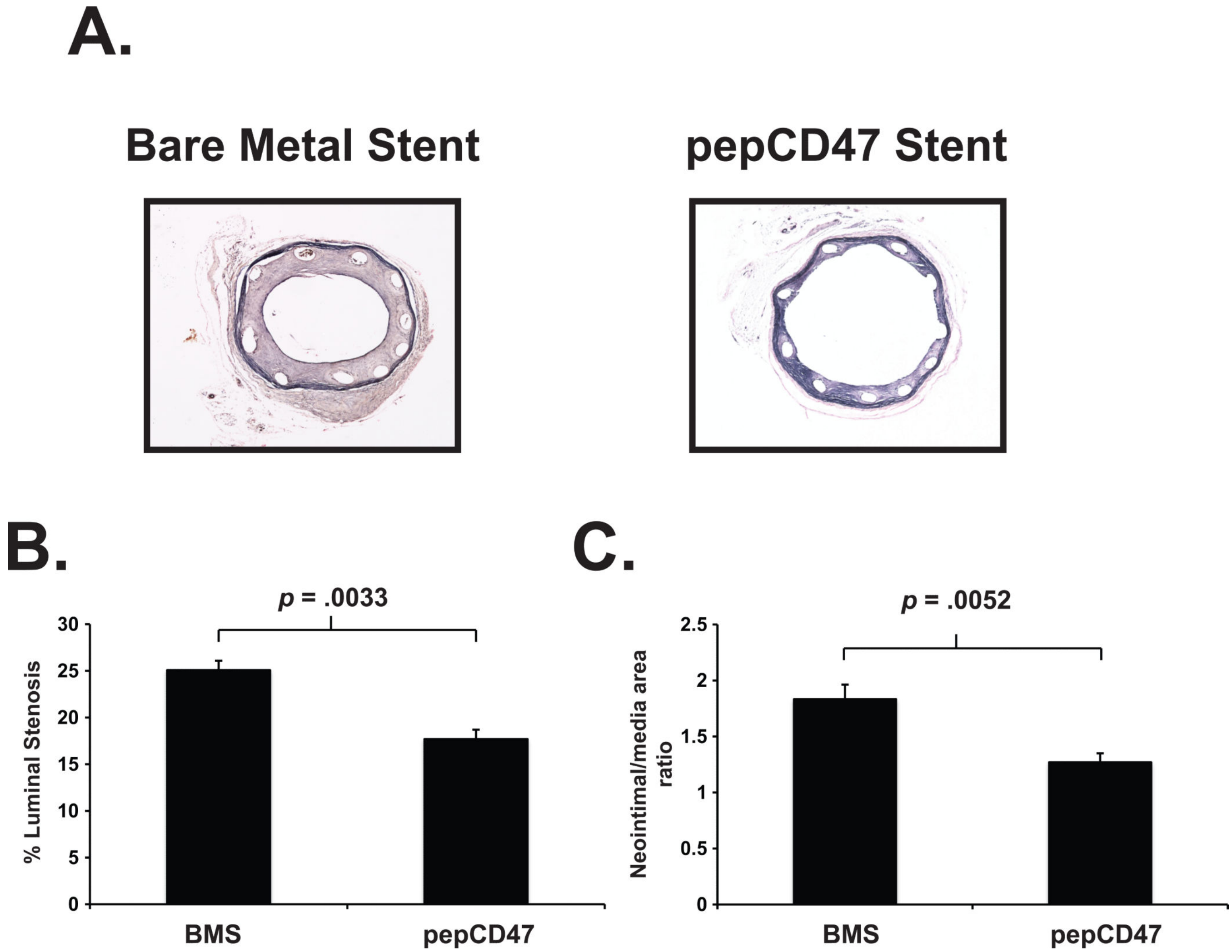

Fig. 8.

The anti-restenotic effect of CD47 modified stents in a rat carotid artery. Bare metal stents or thiolated pepCD47-modified stents were deployed in the carotid artery of rats. The stents were explanted after 14 days. (A) Representative Hematoxylin-eosin stain of explanted stents. Quantitative morphometric analyses of explanted stents demonstrate that (B) luminal stenosis and (C) Neointima/media area ratio are significantly ($p \le 0.05$) reduced as a function of CD47 immobilization. Data represent measurements from 10 individual explanted stents and are presented as mean ± SD.

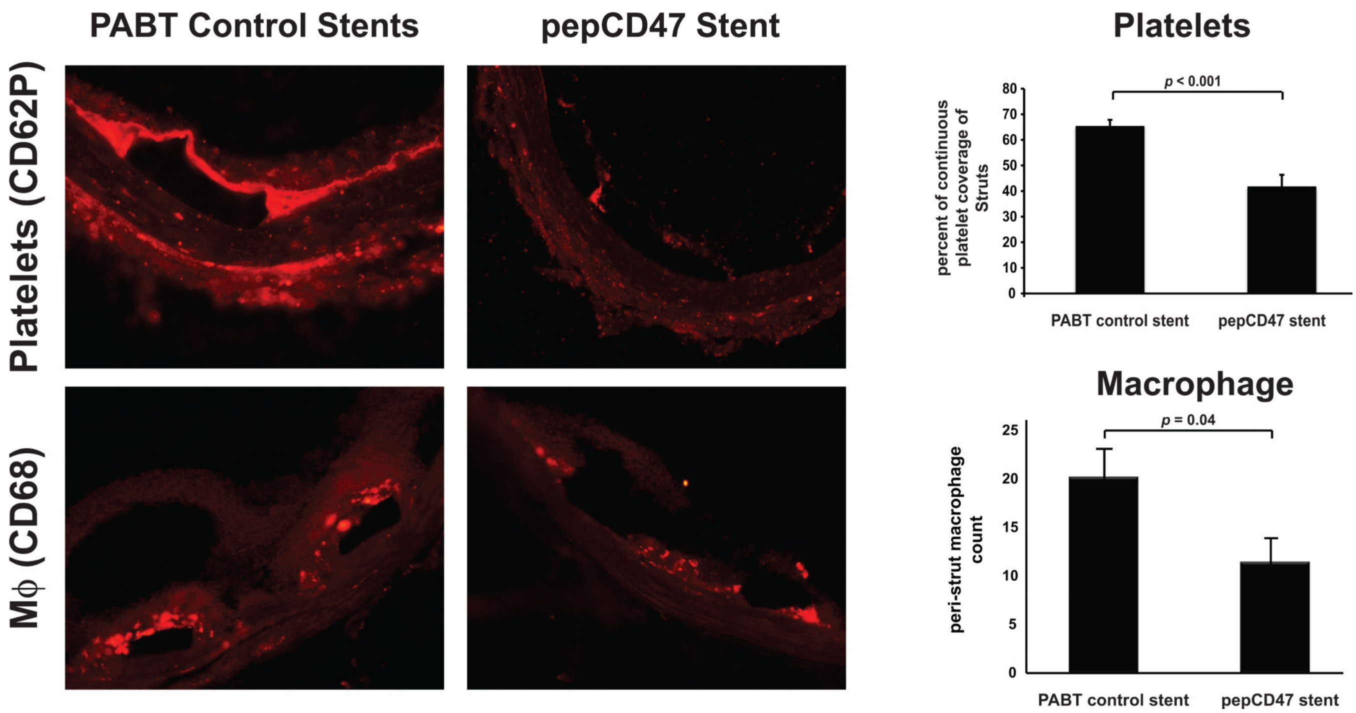

Fig. 9.

Temporal qualitative and quantitative comparisons of cell types from explanted endovascular stents. Representative fluorescent micrographs of explanted bare metal stents, modified with the chemical crosslinker (PABT) or with thiolated pepCD47, stained for surface markers of platelets (CD62P) or macrophages (CD68) after 30 minutes or 3 days respectively showing cellular interactions at the stent strut(s). Scale bar = 100μm. Data represent the mean from 2-3 struts from explanted stents and are presented as mean ± SD.